

# Boiling Heat Transfer in the Quenching of a Hot Tube Under Microgravity

C. J. Westbye\* and M. Kawaji†

University of Toronto, Toronto, Ontario M5S 1A4, Canada  
and

B. N. Antar‡

University of Tennessee Space Institute, Tullahoma, Tennessee 37388

Quenching of a hot tube by injection of a subcooled liquid was investigated under microgravity conditions. Liquid Freon (R-113) was injected at mass fluxes between 160–850 kg/m<sup>2</sup>s into an initially hot, thin-walled stainless steel tube, 11.3 mm i.d. and 914 mm long. Data collected in microgravity aboard NASA's KC-135 aircraft were compared with quenching tests in a horizontal tube under normal gravity. The rewetting temperatures were found to be 15°–25°C lower in microgravity than those obtained under 1 g, and the film boiling heat transfer coefficients in microgravity were only 20–50% of the values obtained in 1 g. This resulted in much longer precursory cooling periods in microgravity, and hence, the time to totally quench the initially hot tube in microgravity was greatly extended. However, once the tube was cooled sufficiently to allow axial propagation of the quench front, the rewetting velocity was found to be slightly greater in microgravity. The boiling curves showed that the nucleate and transition boiling curves in microgravity were shifted to lower wall superheats as compared to 1 g as a result of the lower rewetting temperature. The heat flux profiles were otherwise quite similar, indicating that these boiling regimes are little affected by reduction in gravity.

## Nomenclature

$G$	= mass flux, kg/m <sup>2</sup> s
$h_{fb}$	= film boiling heat transfer coefficient, W/m <sup>2</sup> K
$Q$	= volumetric flow rate, m <sup>3</sup> /s
$q''$	= heat flux, W/m <sup>2</sup>
$q''_{max}$	= maximum heat flux, W/m <sup>2</sup>
$T_l$	= liquid temperature, K
$T_{sat}$	= liquid saturation temperature, K
$T_w$	= wall temperature, K
$z$	= axial coordinate, m
$\Delta T_{sub}$	= liquid subcooling, $T_{sat} - T_l$ , K

## Introduction

THERE are a variety of processes that will occur onboard orbiting space facilities or spacecraft that will involve heat transfer and two-phase liquid–vapor systems. In the refueling of space transfer vehicles with liquid hydrogen/oxygen propellants, or in any transfer and storage of cryogenics, a transient quenching process is expected due to the relatively high initial temperature of the transfer lines and receiving tanks compared to the boiling points of the fluids. Two-phase flow and boiling heat transfer can also occur in the operation of space-based nuclear power reactors.

Research into adiabatic two-phase flows under microgravity ( $\mu g$ ) has received some attention in the past two decades. Studies performed by Heppner et al.,<sup>1</sup> Dukler et al.,<sup>2</sup> and others have primarily focused on the flow patterns that develop and on the two-phase pressure drop. The general conclusion reached from these experiments was that in microgravity the “distributed” flow regimes (such as bubbly and dispersed flow) occur over a wider range of qualities than

under normal gravity (1 g). New flow regimes have also been observed, such as “frothy annular” where the liquid film in annular flow was twice the normal thickness. In these studies extensive use has been made of parabolic aircraft, such as NASA's KC-135, to produce short periods of microgravity. Research on pool boiling under reduced gravity conditions has also received some attention, beginning with the studies by Merte and Clark.<sup>3</sup>

To date, however, there has been very little research into the quenching of a hot surface with a flowing coolant under microgravity. It is known from past studies, including our own work on quenching phenomena in 1 g,<sup>4</sup> that the two-phase flow patterns existing under quenching conditions are quite different from those observed under adiabatic, or even boiling but nonquenching conditions. Typically, in quenching of a vertical tube, inverted annular flow and dispersed flow patterns occur with film boiling heat transfer characteristics that are highly dependent on the hydrodynamics. In horizontal tubes, the liquid flow is asymmetric about the axis due to stratification caused by gravity. The flow patterns that we observed in microgravity during a series of experiments performed aboard the KC-135, have been reported previously<sup>5</sup>: inverted annular and dispersed flow predominated, with a much thicker vapor film layer in the inverted annular regime than was observed in 1 g. This article focuses on the heat transfer behavior and rate of quenching of a hot tube by forced injection of a subcooled liquid coolant.

## Experimental Apparatus

A compact test loop was constructed incorporating a stainless steel (SS 304) tubular test section, liquid reservoir, condenser, and a pump. Figure 1 shows a schematic diagram of this apparatus. The test section was 914 mm long, 11.3 mm i.d., with a wall thickness of 0.71 mm. It was heated to initial temperatures ranging from 200 to 400°C using an ac-powered, insulated electrical heater tape spirally wound externally around the tube. Freon (R-113) was selected as the working fluid, because of its relatively low boiling point (47.6°C) at atmospheric pressure. The subcooled R-113 was injected into the initially hot, dry test section at the beginning of microgravity

Received March 3, 1994; revision received Nov. 15, 1994; accepted for publication Nov. 16, 1994. Copyright © 1995 by the American Institute of Aeronautics and Astronautics, Inc. All rights reserved.

\*Nuclear Design Engineer, Reactor Safety and Operational Analysis Department, Ontario Hydro.

†Professor, Department of Chemical Engineering and Applied Chemistry.

‡Professor of Engineering Science and Mechanics. Member AIAA.

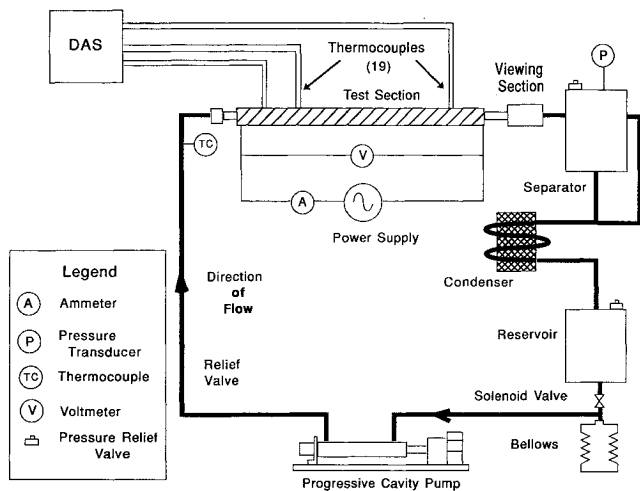


Fig. 1 Schematic diagram of experimental apparatus.

using a progressive cavity pump at flow rates from 160 to 850 kg/m<sup>2</sup>s (10.2 to 54.3 ml/s, measurement uncertainty  $\pm 1$  ml/s). The pump was fed from a collapsible bellows that was isolated from the flow loop using a solenoid valve; this prevented gas or vapor bubbles existing in the reservoir from becoming entrained in the inlet line.

Upon injection, the subcooled freon ( $\Delta T_{\text{sub}} = 17\text{--}24^\circ\text{C}$ ) would immediately vaporize, forming a two-phase liquid-vapor mixture. This mixture flowed through the tube cooling the tube surface, and entered a liquid-vapor separator, a Lucite box with a sufficient volume to prevent substantial overpressurization. The liquid-vapor mixture then flowed from the separator into the condenser, which consisted of a serpentine tube covered externally with heat exchanger fins. Ambient air was forced over these fins using an electric fan. After passing through the condenser, the single-phase liquid was collected and stored in a Lucite reservoir. Following each 20-s period of microgravity, the pump would be switched off and the bellows would be refilled from the reservoir.

The temperature of the test section was monitored using 19 type-K (chromel-alumel) thermocouples, spot-welded to the outside surface of the tube at 11 axial and up to 3 circumferential positions. These thermocouples were placed beneath the insulated ac-heating tape, isolating them from the ambient environment. Signals from these thermocouples, and from other instrumentation including a thermocouple monitoring the liquid temperature and a triple-axis accelerometer, were sampled at a rate of 10 Hz using a personal computer equipped with a DAS-8 data acquisition card multiplexed to two MUX-16 expansion boards. It was estimated that the accuracy of the temperature measurements was  $\pm 2^\circ\text{C}$ . The locations and designations for each thermocouple are shown in Fig. 2.

The KC-135 provides about 40 parabolas during which the downward acceleration is less than  $\pm 2\%$  of normal gravity for a period of about 20 s. Before reaching each microgravity period, the heater was switched on and the tube was heated to an initial temperature greater than  $200^\circ\text{C}$ . At the start of microgravity, the heater was switched off and the progressive cavity pump was activated, flooding the tube with subcooled liquid. The data acquisition system operated continuously throughout the flight, and video camcorders recorded the flow patterns in the separator and in a viewing section (a transparent tube) located between the exit of the test section and separator. Following microgravity, liquid injection continued until the tube temperature had been reduced to a low, uniform value, at which time the pump was turned off and the heater switched back on. This was necessary to ensure that the initial axial temperature profile of the tube was uniform; during some runs in which the quench front only partially propagated

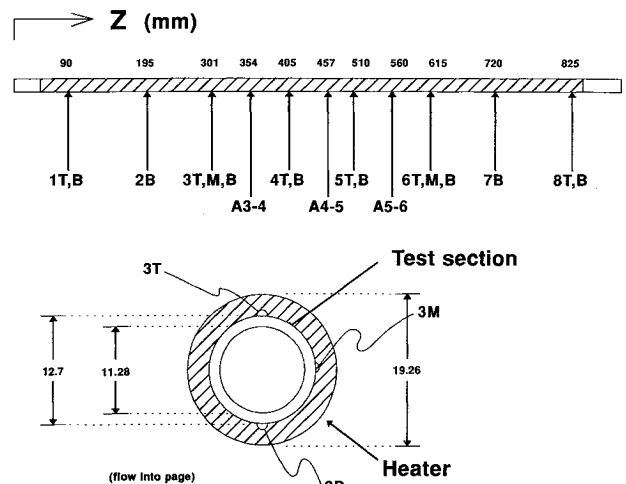


Fig. 2 Thermocouple locations and designations, all dimensions in millimeters.

along the tube, the inlet region became quenched (reduced to a low temperature) while the outlet region remained at a much higher temperature. Since the heater power was limited, alternate parabolas had to be skipped to allow the tube to uniformly heat up to the desired initial temperature.

## Results

Experiments were performed on the ground with the tube oriented horizontally to provide comparison data for the microgravity experiments. To allow direct comparison, it was desired to perform the 1 g and  $\mu\text{g}$  experiments with the same boundary conditions: initial tube temperature, liquid subcooling, and flow rate. The initial tube wall temperature imposed during the microgravity tests was selected to allow the majority of the test section to quench within the time available (20 s). However, it was found that the rewetting temperature (the wall temperature at which direct liquid-surface contact is established and maintained) was higher in 1 g than in  $\mu\text{g}$ : when the same initial tube wall temperature was used in 1 g, the tube became rewetted immediately upon injection. Hence, in some cases the initial temperature used in 1 g was set higher than the corresponding  $\mu\text{g}$  run.

### Tube Wall Temperature Response

Typical temperature transients during rewetting in  $\mu\text{g}$  and 1 g are shown in Figs. 3 and 4, respectively. These temperature profiles were taken at the outer bottom surface of the tube, but because the tube was thin-walled, they are very close to the inner surface temperatures. Using the solution to the transient inverse heat conduction problem,<sup>6</sup> it was estimated that the difference between the inner and outer wall temperatures was generally less than  $1^\circ\text{C}$ , except when the temperature was falling rapidly, in which case the difference was about  $5^\circ\text{C}$ . As mentioned above, the uncertainty in the measured temperature due to thermocouple noise was  $\pm 2^\circ\text{C}$ .

The tube wall temperature was gradually reduced from its high initial value through the process of film boiling, where only Freon vapor was in contact with the tube wall. Previous experiments performed with a transparent quartz tube showed that the flow pattern under both gravity levels was either inverted annular or dispersed flow. Once the wall temperature had been reduced to the rewetting temperature, the liquid was able to come into direct contact with the wall surface, and the rate of heat removal was greatly increased as demonstrated by the rapid temperature reduction at the "knee" of the temperature curve. The prevailing boiling regimes at the quench front are transition boiling, with intermittent liquid-surface contact, and then nucleate boiling once direct liquid-wall contact is fully established.

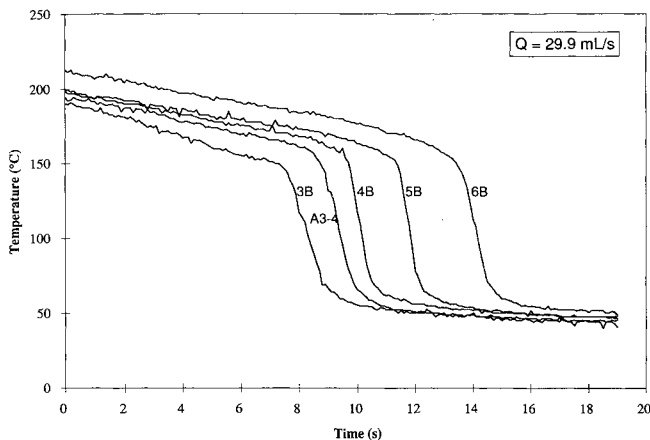


Fig. 3 Transient temperature profiles at various axial locations in  $\mu g$ .

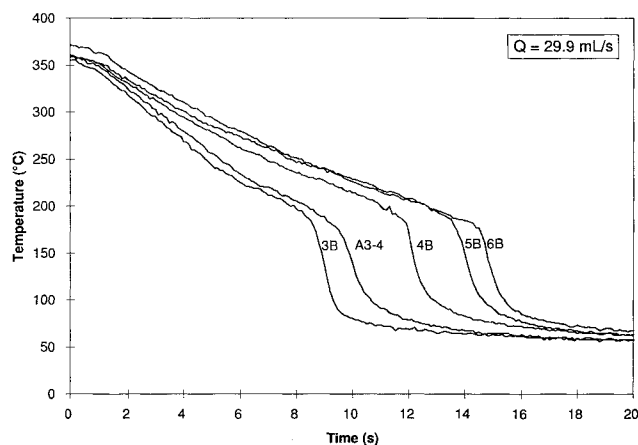


Fig. 4 Transient temperature profiles at various axial locations in 1 g.

One difference between quenching behavior in microgravity and normal gravity is illustrated in Figs. 3 and 4: even though the initial tube temperature is about 150°C higher for the 1-g run, the tube becomes "quenched" (reduced to a low temperature) at a given axial location in about the same time as the corresponding  $\mu g$  run. Had these runs been performed using the same initial wall temperature, the tube would have been quenched in significantly less time under 1-g conditions, demonstrating much smaller precursory cooling rates under microgravity that delay the initiation of quenching.

Figure 5 compares the tube temperature response at a single axial location in both 1 g and  $\mu g$ , which demonstrates the symmetry of the flow and heat transfer rates about the tube axis under microgravity conditions: the wall temperature is reduced at the same rate at the top, middle, and bottom of the tube under  $\mu g$ . The same is not true under 1 g: the bottom cools much more rapidly than the middle, which cools more rapidly than the top. This is a result of flow stratification caused by gravity in a horizontal tube, as depicted in the inset diagram. The larger vapor film thickness under microgravity, as mentioned above, is also shown schematically in this diagram. Note also that in the run performed under normal gravity, there is no appreciable film boiling regime and the quench front arrives at this downstream axial location immediately upon coolant injection.

#### Rewetting Temperature

The definition of the rewetting temperature (or quench temperature) used in this study is the same as the "apparent rewetting temperature" used by Chen et al.<sup>7</sup> Tangents were

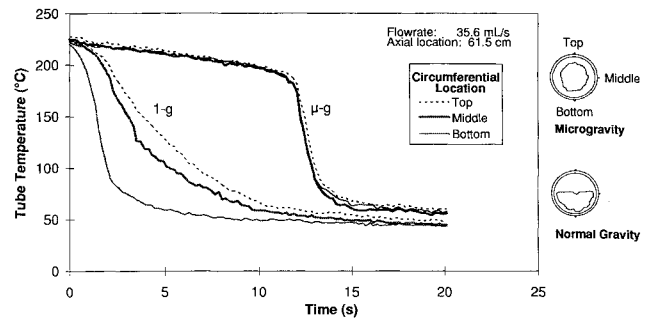


Fig. 5 Transient temperature profiles at three circumferential locations in  $\mu g$  and 1 g. The diagram depicts the flow stratification in 1 g, and the axial symmetry in microgravity.

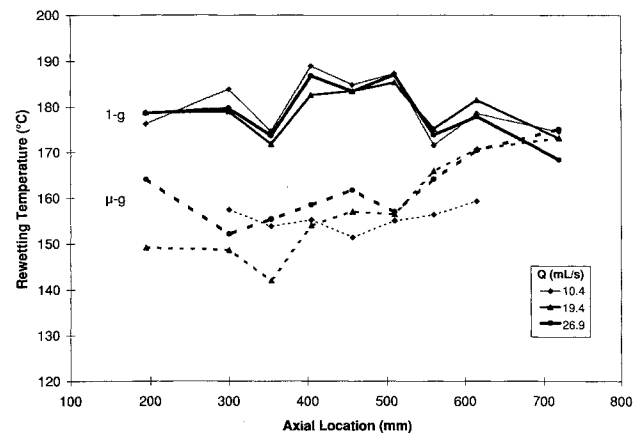


Fig. 6 Axial variation in rewetting temperature in  $\mu g$  and 1 g.

drawn on the transient temperature profiles from the film boiling and transition boiling regimes, with the point of intersection defining the rewetting temperature and the "rewetting time," the time at which the quench front arrives at the axial location under consideration. The axial variation in the rewetting temperature at the bottom of the tube is shown in Figure 6 for several flow rates in both 1 g and  $\mu g$ .

This figure clearly shows that the rewetting temperature is lower in  $\mu g$  than for the same conditions during horizontal flooding under 1 g. Due to variations in the measured rewetting temperatures at different axial locations, no clear axial trend is apparent in Fig. 6. Hence, the rewetting temperature was axially averaged for each flow rate, and the result is shown in Fig. 7. The rewetting temperature was found to be lower in microgravity for all flow rates, with the difference largest (about 25°C) at low flow rates (160 kg/m<sup>2</sup>s), and decreasing to 15°C at the highest flow rate examined, 850 kg/m<sup>2</sup>s. The rewetting temperature was observed to increase with increasing flow rate under both gravity levels. These results are consistent with an interfacial instability model for surface rewetting as described below.

When two phases are in relative motion with respect to one another, a Kelvin-Helmholtz type instability will occur at the gas-liquid interface if the relative velocity is sufficiently large. The amplitude of interfacial waves will grow until the liquid contacts the tube surface. If the surface temperature is high enough, more vapor will be generated that will push the liquid away from the surface and the surface becomes dry again. However, if the tube wall has been reduced to a sufficiently low temperature, continuous liquid-surface contact would be established.

The above model for surface rewetting in horizontal tubes in 1 g has been proposed by Chan and Banerjee<sup>8</sup> and Abdul-Razzak et al.<sup>9</sup> They showed that the model predictions agree well with their rewetting data. According to the model, an

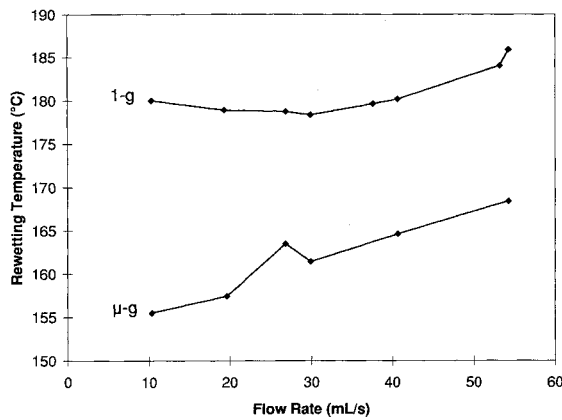


Fig. 7 Axially averaged rewetting temperature as a function of flow rate in  $\mu g$  and 1 g.

increase in the vapor film thickness in inverted annular flow will result in more stable film boiling and will tend to decrease the rewetting temperature. The reduction in rewetting temperature in  $\mu g$  is therefore a result of the larger vapor film thickness. Increasing the liquid flow rate leads to increased instability in the vapor-liquid interface, which leads to the higher rewetting temperatures at high flow rates that were observed. It is also apparent from Fig. 7 that the rewetting temperature increases more rapidly with the liquid injection rate in microgravity as compared to 1-g tests. This indicates that, in the absence of gravitational force, inertial effects become relatively more important, as would be expected.

#### Quench Front Propagation

Another parameter of interest is the speed at which the quench front propagates once the inlet has become quenched. This was obtained by plotting the quench front location against the quench time and evaluating the slope of the curve. In general, it has been found<sup>8,9</sup> that the quench speed is fairly constant axially, and this was also true in this work. The quench speeds obtained are shown in Fig. 8 as a function of liquid injection rate along with the liquid injection velocity. This figure indicates that the quench speeds are much lower than the liquid injection velocity for both gravity levels, and slowly increases with increasing injection rate. This trend is consistent with higher local subcooling at the quench front caused by the higher flow rate, resulting in an increased rewetting velocity; similar results have been previously reported (e.g., Piggott and Duffey<sup>10</sup>). At low injection rates, the quench speeds are similar between 1 g and  $\mu g$ , but interestingly as the flow rate is increased, the rewetting velocity in  $\mu g$  increases more rapidly than in the corresponding runs under 1 g.

In  $\mu g$ , the tube is cooled down significantly before the quench front starts to propagate from the tube inlet and once the quenching process is initiated, the quench front can propagate quickly because the tube wall temperature is low enough to immediately establish liquid-surface contact. Since there is a significant amount of heat transferred to the coolant when the tube wall temperature drops rapidly from the rewetting temperature to near saturation temperature, a large amount of vapor can be generated if the quench front propagates rapidly. This means that, in microgravity, if the liquid injection rate is high, the heat stored in the tube wall can be released in a short time after the initiation of quench front propagation, and a large amount of vapor can be generated that can unexpectedly cause overpressurization of the flow system. It is also noted here that the quench speeds shown in Fig. 8 for the  $\mu g$  and 1-g runs were not obtained using the same initial tube temperature. Chen et al.<sup>7</sup> and others have shown that the quench speed decreases with increasing initial wall temperature, and since the initial temperature for the 1-

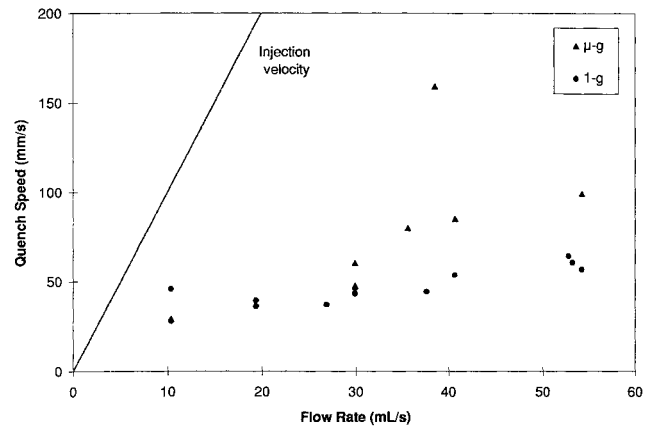


Fig. 8 Quench speed vs flow rate for 1-g and  $\mu g$  runs.

g runs was typically 100°C higher than the corresponding  $\mu g$  run, it may not be surprising to obtain higher quench speeds under  $\mu g$  than 1 g. Nevertheless, significant delays in the initiation of quenching and subsequent rapid propagation of the quench front under microgravity are important factors to consider in future designs of space systems.

#### Boiling Heat Transfer

In order to calculate heat transfer data from the transient temperature profiles, an energy balance was performed. The change in stored heat in a differential element of the tube was equated to the heat transported to the fluid, minus losses to the environment. A computer program was then used to evaluate the transient heat flux to the fluid, and the heat transfer coefficient was calculated assuming that the fluid was at saturation conditions.<sup>11</sup> The approximate error in the calculated heat flux, considering uncertainties in the measurements and limitations of the model, was estimated to be  $\pm 15\%$  in the film boiling regime and  $\pm 5\%$  in the nucleate boiling regime.

A typical heat flux profile generated using this method, based on a temperature transient at the bottom of the tube under 1 g, is shown in Fig. 9 together with the definitions of the three boiling regimes. As shown in this figure, the heat flux in the film boiling regime was relatively constant, as has previously been observed.<sup>7</sup> This prompted the use of a time-averaged value for the film boiling heat transfer coefficient  $h_{fb}$  to facilitate comparison between 1 g and  $\mu g$ . The results of this calculation are shown in Fig. 10, where  $h_{fb}$  at the bottom of the tube is plotted against axial location for two flow rates in 1 g and  $\mu g$ .

In both cases, it was observed that the film boiling heat transfer coefficient decreased with increasing axial location, and increased with increasing flow rate. Both of these trends can be related to the change in local liquid subcooling. Chen et al.<sup>7</sup> have shown that  $h_{fb}$  increases with increasing subcooling; hence, at the inlet of the tube where the subcooling is largest,  $h_{fb}$  is at a maximum value. Similarly, at high flow rates the residence time of the liquid in the test section is reduced, resulting in less heating of the liquid and higher subcooling, which increases  $h_{fb}$ . There could also be an increase in convective heat transfer at high flow rates, which contributes to the increase in  $h_{fb}$ .

While  $h_{fb}(z)$  shows the same parametric trends in both 1 g and  $\mu g$ , Fig. 10 clearly shows that the value of  $h_{fb}$  in  $\mu g$  is substantially less than the corresponding 1-g value. This is demonstrated for a variety of flow rates in Fig. 11, where the ratio of  $h_{fb}$  in  $\mu g$  to  $h_{fb}$  in 1 g is plotted as a function of axial location. This ratio varied from a minimum of about 0.15 for the lowest flow rate, to about 0.60 at high flow rates. Two trends are evident from this figure. First, the ratio generally tends to increase with axial distance, indicating that gravity

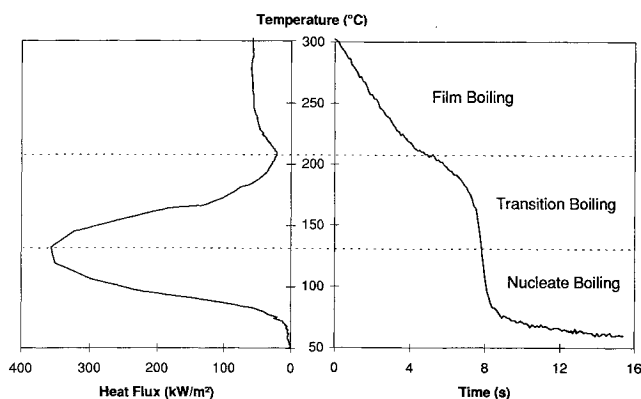
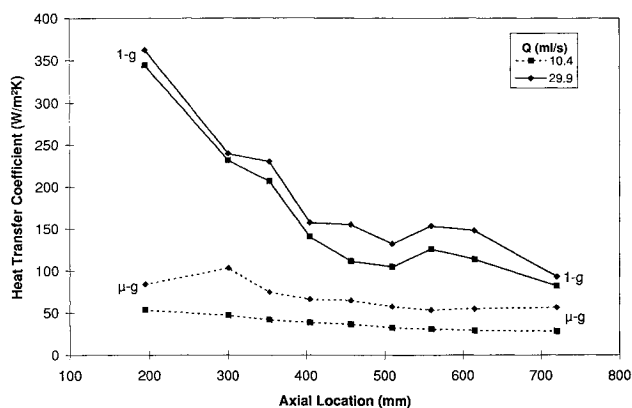
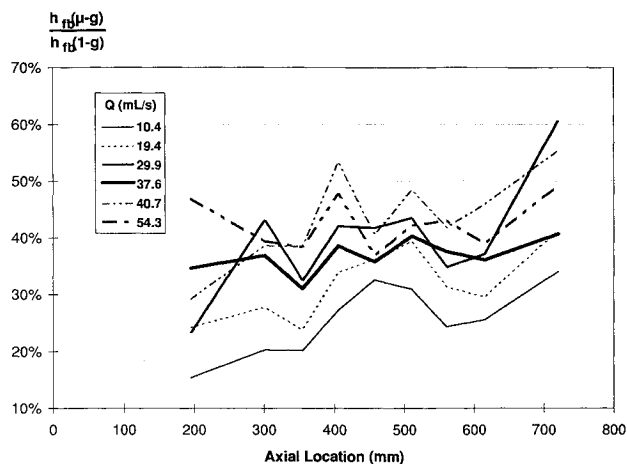


Fig. 9 Definition of boiling regimes.

Fig. 10 Axial variation of  $h_{fb}$  for two flow rates in 1 g and  $\mu$ g.Fig. 11 Ratio of film boiling heat transfer coefficients in  $\mu$ g to 1 g for various flow rates.

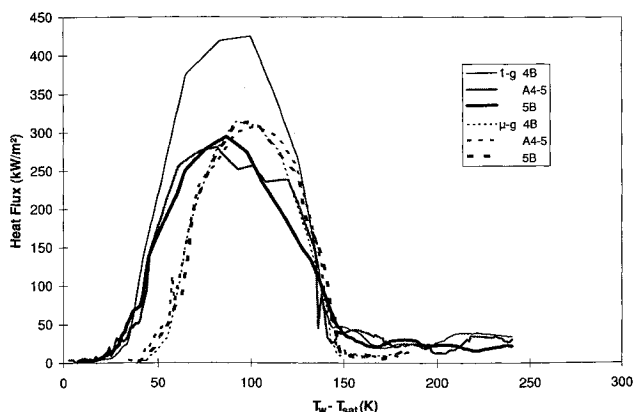
becomes less important far from the inlet. This is possibly a result of thicker vapor films far from the inlet, caused by higher vapor generation rates as the local subcooling is reduced. Second, the ratio generally increases with flow rate. This is another example of inertial effects becoming relatively more important in the absence of gravity; in the limit of very high flow rates, it is expected that the ratio would approach unity.

This dramatic reduction in film boiling heat transfer coefficient in microgravity, typically by a factor of 2–5, slows down the rate of heat removal from the tube wall during film boiling, which greatly extends the time required to completely quench the hot tube. This could have serious implications in the operation of space systems because the time required to

reduce the temperature of heater elements from above the rewetting temperature would be much greater than under 1 g. This result also has similar implications for the design of cryogen transfer systems, and the other applications mentioned in the Introduction. However, it should be noted that once the tube temperature is reduced to the liquid rewetting temperature, the quench front propagates at about the same speed as on the ground or even faster. If the quench speed is actually higher in microgravity than in 1 g, this could lead to rapid vapor generation and overpressurization of the system as mentioned previously, which can possibly cause failure of the pipes and vessels in the system.

Following the collapse of a vapor film in film boiling, the heat flux increases sharply through the transition boiling regime and reaches a maximum. The heat flux then decreases with decreasing wall superheat through the nucleate boiling regime, as shown in Fig. 9. It was found, in keeping with previous results, that the heat flux in the nucleate boiling regime was independent of both axial location and coolant flow rate. Since nucleate boiling occurs immediately upstream of the quench front, and since the liquid layer close to the quenched surface will be very close to saturation temperature at this location, liquid subcooling was thought to have little effect in this boiling regime. Heat flux data for the transition boiling regime showed considerable scatter (10–20% among different axial locations for a given run and among different runs at the same axial location) due to the rapidity of the temperature transient compared to the data acquisition rate. Typically, the tube temperature at a given location dropped rapidly after rewetting and the number of temperature data points collected during this transition boiling regime was considerably smaller compared to that for film and nucleate boiling regimes. Since the heat flux values had to be calculated from the slope of the temperature data using the inverse conduction theory, larger uncertainties incurred in the slope of the temperature profile resulted in greater scatter in the calculated heat flux.

A comparison of the heat flux profiles, as a function of wall superheat ( $T_w - T_{sat}$ ), in both  $\mu$ g and 1 g for several axial locations, is shown in Fig. 12. The only difference between the profiles in 1 g and  $\mu$ g is due to the lower rewetting temperature in  $\mu$ g: the boiling curves in microgravity are shifted towards lower wall superheats, and have a smaller width. However, once surface rewetting is initiated, similar heat flux profiles are obtained. The nucleate boiling heat fluxes have virtually identical slopes for all axial locations, indicating that the nucleate boiling regime is unaffected by gravity level. This result is consistent with the pool boiling results from previous experiments.<sup>3,12</sup> Although the heat flux values have a greater uncertainty, the transition boiling curves obtained in  $\mu$ g and 1 g are also similar, indicating that this regime is probably not overly sensitive to gravity level either.

Fig. 12 Boiling curves in 1 g and  $\mu$ g for  $Q = 19.4$  ml/s.

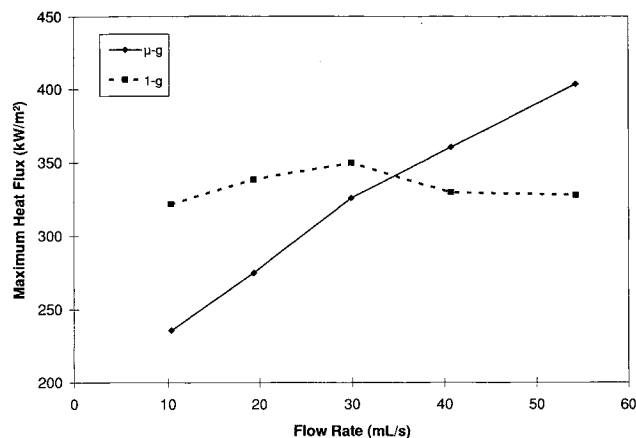


Fig. 13 Variation of axially averaged maximum heat flux with flow rate.

Another parameter of interest is the maximum heat flux ( $q''_{\max}$ ). These were obtained by inspection from the boiling curves, and plotted as a function of axial location. No definite trend could be established with respect to axial location, and so the maximum heat flux was axially averaged to allow more direct comparison. The axially averaged maximum heat fluxes obtained in 1 g and  $\mu$ g are shown as a function of flow rate in Fig. 13. In general,  $q''_{\max}$  was observed to increase with increasing flow rate, as has been reported in the literature. This trend did not hold for the 1-g tests at the highest flow rate, and this was thought to be a result of slightly ( $3^{\circ}\text{C}$ ) lower subcooling for these runs; it has been reported<sup>7,13</sup> that the maximum heat flux decreases with decreasing subcooling.

It can be seen from Fig. 13 that at low flow rates the maximum heat flux is lower in microgravity than in 1 g. This is consistent with the results of Merte and Clark,<sup>3</sup> who found that  $q''_{\max}$  was substantially reduced during pool boiling ( $Q = 0$ ) under microgravity. An unexpected finding, however, was that the maximum heat flux increased more quickly with flow rate in  $\mu$ g than in 1 g, so that at a certain flow rate ( $Q \approx 35$  ml/s, or  $G \approx 500$  kg/m<sup>2</sup>s) the maximum heat fluxes became equal, and at higher flow rates  $q''_{\max}$  was actually larger in  $\mu$ g than in 1 g. No satisfactory physical explanation for this phenomenon has yet been determined and further measurements using micro heat flux sensors are currently underway.

### Conclusions

An experimental investigation to determine the effect of reduced gravity on the rewetting of a tube and flow boiling of R-113 has been described. It was found that due to a large vapor film thickness, the rewetting temperature is reduced in microgravity by about 15 to  $25^{\circ}\text{C}$  compared to similar tests performed using a horizontal tube in 1 g, with the difference decreasing with increasing liquid flow rate. The parametric trends affecting the rewetting temperature support a Kelvin-Helmholtz instability model for the rewetting of hot surfaces.

The rate of heat transfer in the film boiling mode has been found to be greatly reduced under microgravity conditions. The film boiling heat transfer coefficient in  $\mu$ g was typically only 20 to 50% of its 1-g value, with the ratio increasing with increasing flow rate. This reduction in percursory cooling rates leads to a dramatic increase in the time required to cool the

tube to initiate the quench front propagation. However, once the quench front starts to propagate from the inlet, it propagated at about the same speed as in 1 g, or even faster.

The nucleate (and possibly transition) boiling in flow boiling conditions was found to be insensitive to gravity levels. The maximum heat flux was observed to be lower in microgravity at low flow rates ( $G < 500$  kg/m<sup>2</sup>s), and higher than the corresponding 1-g values at high flow rates. These results indicate that conventional correlations derived using data obtained on the ground will be inadequate to fully describe heat transfer involved in quenching processes in space systems, and some care should be exercised in designing future systems.

### Acknowledgments

The authors would like to thank the Canadian Space Agency and the Natural Sciences and Engineering Research Council of Canada for providing the financial support and KC-135 flight opportunities for this work.

### References

- Heppner, D. B., King, C. D., and Littles, J. W., "Zero-G Experiments in Two-Phase Fluids Flow Regimes," American Society of Mechanical Engineers Paper 75-ENAS-24, 1975.
- Dukler, A. E., Fabre, J. A., McQuillen, J. B., and Vernon, R., "Gas-Liquid Flow at Microgravity Conditions: Flow Patterns and Their Transitions," *International Journal of Multiphase Flow*, Vol. 14, No. 4, 1988, pp. 389-400.
- Merte, H., Jr., and Clark, J. A., "Boiling Heat Transfer with Cryogenic Fluids at Standard, Fractional, and Near-Zero Gravity," *Journal of Heat Transfer*, Vol. 86, Aug. 1964, pp. 351-359.
- Kawaji, M., Ng, Y. S., Banerjee, S., and Yadigaroglu, G., "Reflooding with Steady and Oscillatory Injection," *Journal of Heat Transfer*, Vol. 107, No. 3, 1985, pp. 670-678.
- Kawaji, M., Westbye, C. J., and Antar, B. N., "Microgravity Experiments on Two-Phase Flow and Heat Transfer During Quenching of a Tube and Filling of a Vessel," *27th AIChE Symposium Series*, Vol. 87, No. 283, 1985, pp. 236-243.
- Burggraf, O. R., "An Exact Solution of the Inverse Problem in Heat Conduction Theory and Applications," *Journal of Heat Transfer*, Vol. 86, Series C, Aug. 1964, pp. 373-382.
- Chen, W. J., Lee, Y., and Groeneveld, D. C., "Measurement of Boiling Curves During Rewetting of a Hot Circular Duct," *International Journal of Heat and Mass Transfer*, Vol. 22, No. 6, 1979, pp. 973-976.
- Chan, A. M. C., and Banerjee, S., "Refilling and Rewetting of a Hot Horizontal Tube—Part I: Experiments," *Journal of Heat Transfer*, Vol. 103, May 1981, pp. 281-286.
- Abdul-Razzak, A., Shoukri, M., and Chan, A. M. C., "The Dynamic Behavior of Liquid-Vapor Interface During Film Boiling in Horizontal Tubes and Its Role in Surface Rewetting," *Phase-Interface Phenomena in Multiphase Flow*, edited by G. F. Hewitt, F. Mayinger, and J. R. Riznic, Hemisphere, New York, 1991, pp. 131-143.
- Piggott, B. D. G., and Duffey, R. B., "The Quenching of Irradiated Fuel Pins," *Nuclear Engineering and Design*, Vol. 32, 1975, pp. 182-190.
- Westbye, C. J., "Flow Boiling Heat Transfer in the Quenching of a Hot Tube Under Microgravity Conditions," M.A.Sc. Thesis, Dept. of Chemical Engineering and Applied Chemistry, Univ. of Toronto, Toronto, Ontario, Canada, 1992.
- Zell, M., Straub, J., and Vogel, B., "Pool Boiling Under Microgravity," *PhysicoChemical Hydrodynamics*, Vol. 11, Nos. 5/6, 1989, pp. 813-823.
- Cheng, S. C., Ng, W. L., and Heng, K. T., "Measurements of Boiling Curves of Subcooled Water Under Forced Convective Conditions," *International Journal of Heat and Mass Transfer*, Vol. 21, No. 11, 1978, pp. 1385-1392.